JAM CM Journal of Applied Mathematics and Computational Mechanics 2026, 25(1), 86-97
www.amcm.pcz.pl p-ISSN 2299-9965
DOI: 10.17512/jamcm.2026.1.08 e-ISSN 2353-0588

MODELING THE EFFECT OF CARBON BLACK TYPE AND DOSAGE ON THE MIXING DYNAMICS OF RUBBER BLENDS USING A GENERAL REGRESSION NEURAL NETWORK

Ivan Kopal[1], Juliána Vršková[1], Ivan Labaj[1], Marta Harničárová[2, 3], Jan Valíček[2, 3]

[1] Faculty of Industrial Technologies in Púchov, Alexander Dubček University of Trenčín
Púchov, Slovak Republic
[2] Faculty of Engineering, Slovak University of Agriculture in Nitra
Nitra, Slovak Republic
[3] Faculty of Technology, Institute of Technology and Business in České Budějovice
České Budějovice, Czech Republic
ivan.kopal@tnuni.sk, juliana.vrskova@tnuni.sk, ivan.labaj@tnuni.sk, marta.harnicarova@uniag.sk
jan.valicek@uniag.sk, harnicarova@mail.vstecb.cz, valicek.jan@mail.vstecb.cz

Received: 14 October 2025; Accepted: 4 February 2026

Abstract. This study presents the application of a general regression neural network to model the effects of carbon black type and content on the mixing dynamics of rubber blends. The neural network model, trained on data from 16 tests (four carbon black types with contents of 45-60 phr), accurately reconstructs the torque and temperature profiles during blend mixing. Model optimization was performed using 10-fold cross-validation. The simulation results (average $R^2 \approx 1$ and RMSE $\approx 10^{-4}$) confirm the practical applicability of the presented model for predicting the time evolution of nonlinear processes in complex technological applications.

MSC 2010: *97R40, 62Q99*
Keywords: *rubber blends, carbon black, mixing dynamics, artificial neural networks, general regression neural networks*

1. Introduction

Rubber mixing is a complex technological process that requires precise control of ingredient dosing and mixing dynamics. Reinforcing fillers, particularly carbon black (CB), significantly influence the rheological behavior of the blend and thereby affect both processing and final product quality [1, 2]. However, the addition of fillers introduces nonlinear interactions within the blend during mixing, which traditional analytical methods cannot reliably capture. Mixing process monitoring is commonly based on torque and temperature time histories, reflecting the evolving interactions among blend constituents under specific conditions [1-3].

Artificial intelligence, especially artificial neural networks (ANNs), has recently gained importance for modeling such dynamic processes using historical data [4-9]. Among them, the general regression neural network (GRNN) stands out due to its fast learning, strong noise tolerance, and excellent handling of nonlinearities [10-12]. Despite its suitability, GRNN has so far seen virtually no application in rubber mixing processes.

The aim of this study was to develop and experimentally validate a GRNN model capable of simulating the time evolution of torque and temperature during the mixing of natural rubber-based blends with various types and concentrations of CB.

2. Materials and methods

2.1. Blend preparation and computational setup

GRNN was applied to natural rubber (NR) blends filled with four CB types – N121, N339, N550, and N660 – at concentrations of 45, 50, 55, and 60 phr. Sixteen unique formulations were tested, generating 32 torque and temperature curves. Full blend compositions, component functions, and suppliers are provided in Table 1.

Table 1. Composition of the natural rubber-based blend used in this study, including the function and supplier of each component

Component	Content [phr]	Function	Supplier
Natural rubber grade 1500	100	Matrix	Synthos Kralupy a.s., Kralupy nad Vltavou, CZ
Carbon black type N121, N339, N550, N660 (CB)	45:5:60	Filler	Makrochem Sp. z o.o., Lublin, PL
Zinc oxide (ZnO)	3	Vulcanization activator	SlovZink a.s., Koseca, SK
Stearic acid	1	Vulcanization activator	Setuza a.s., Ústí nad Labem, CZ
Sulfur Crystex OT33 (S)	1.75	Vulcanizing agent	Eastman Chemical Company, Kingsport, TN, USA
TBBS	1	Vulcanization accelerator	Duslo a.s., Šaľa, SK

The blends were prepared in a Brabender Plastograph EC Plus laboratory mixer (Brabender GmbH & Co. KG, Duisburg, Germany) with an 80 cm^3 chamber, following a single-stage procedure according to ISO 2393 [13] and using a fill factor of 0.65-0.85. NR was masticated at 90 ±1 °C under a 5 kg ram load and a rotor blade speed of 50 ±1 rpm for 3 min. ZnO and stearic acid were then sequentially incorporated and mixed for 45 s and 30 s, respectively, followed by CB, which was mixed for 3 min. Finally, S and TBBS were added and mixed for 1.5 min.

Torque and temperature of the blend were continuously recorded every 2 s using automatically calibrated sensors (±0.1 Nm, ±0.5 °C). Each formulation was prepared and tested five times under strictly controlled laboratory conditions (23 ±2 °C, 101.3 ±2 kPa, 50 ±5 % RH), ensuring reproducibility. The variability of torque and temperature did not exceed ±5 % and ±1.5 °C, respectively. Accurate dosing of all components was maintained with a Mettler Toledo XS205 balance (±0.01 g; Mettler Toledo International Inc., Columbus, OH, USA), ensuring precise formulation.

The GRNN model was implemented in MATLAB® R2022a (version 9.12, 64-bit; MathWorks, Natick, MA, USA) using the Neural Network Toolbox and Statistics and Machine Learning Toolbox.

2.2. Data preprocessing

The torque **M** and blend temperature **T** as functions of the mixing time **t** were recorded from each experiment. The obtained data for each CB type and its concentration in the blend were organized into tables representing data structures in the form of matrices composed of column vectors:

$$\begin{gathered}\boldsymbol{\zeta}^{(p)} = \mathrm{concat}_{q=1}^{Q}\left[C^{(q)} \cdot \mathbf{1}_{n_q} \;\; \mathbf{t}^{(q)} \;\; \boldsymbol{\Theta}^{(q)}\right] \in \mathbb{R}^{N\times 3}, \\ \boldsymbol{\zeta}^{(p)} \in \left\{\boldsymbol{\mu}^{(p)}, \boldsymbol{\tau}^{(p)}\right\}, \;\; \boldsymbol{\Theta}^{(q)} \in \left\{\mathbf{M}^{(q)}, \mathbf{T}^{(q)}\right\}, \;\; N = \sum_{q=1}^{Q} n_q,\end{gathered} \tag{1}$$

where N is the total number of records across all concentrations q for CB type p; n_q is the number of samples in the test with a q value for a given p; p = 1, 2, ... P is the index of the CB type; q = 1, 2, ... Q is the CB concentration index; $C^{(q)}$ is the concentration of the CB in a given test; $\mathbf{1}_{n_q}$ is the unit vector of length n_q used to replicate the value of $C^{(q)}$ into a vector of length $\mathbf{t}^{(q)}$; $\mathbf{t}^{(q)}$, $\mathbf{M}^{(q)}$ and $\mathbf{T}^{(q)}$ are the time series of time, torque, and temperature values for a given mixing cycle; and the concat operator represents the vertical chaining (concatenation) of the matrix blocks.

The generated matrix tables $\boldsymbol{\mu}^{(p)}$ and $\boldsymbol{\tau}^{(p)}$ were then arranged in a single-line cell array-type data structure of the following form:

$$W = \left(\left\{\boldsymbol{\mu}^{(p)}\right\}_{p=1}^{P} \parallel \left\{\boldsymbol{\tau}^{(p)}\right\}_{p=1}^{P}\right) \in (\mathbb{R}^{N\times 3})^{2P}, \tag{2}$$

where the symbol ‖ represents the ordered chained union operator of the two matrix sequences. This flexible data structure represents the basic framework for further processing of registered data.

All incomplete and erroneous records were removed from the W structure. The raw data were not additionally filtered or smoothed to preserve local fluctuations and inequalities, allowing the model to better reflect complex mixing dynamics and increase robustness to noise. Conversely, their suppression could lead to a loss of information regarding the incorporation progress of the blend components, which is important for the successful generalization of the model to real data.

From each matrix $\boldsymbol{\mu}^{(p)}$ and $\boldsymbol{\tau}^{(p)}$ in the cell array W, the input $\mathbf{x}^{(p,q)}$ and target $\mathbf{y}^{(p,q)}$ data for the model were extracted for each combination of indices p and q:

$$\begin{gathered}\mathbf{x}^{(p,q)} = \left[C^{(q)} \cdot \mathbf{1}_{n_q} \;\; \mathbf{t}^{(q)}\right] \in \mathbb{R}^{n_q \times 2}, \\ \mathbf{y}_{\mathrm{M}}^{(p,q)} = \mathbf{M}^{(q)} \in \mathbb{R}^{n_q \times 1}, \;\; \mathbf{y}_{\mathbf{T}}^{(p,q)} = \mathbf{T}^{(q)} \in \mathbb{R}^{n_q \times 1},\end{gathered} \tag{3}$$

where the input matrices contain the CB concentration and mixing time, and the target matrices represent the torque and temperature values of the blend, respectively.

The input and target data were normalized to the range $\langle 0, 1\rangle$ as follows [14]:

$$\begin{gathered}\boldsymbol{\xi} = \frac{\mathbf{z}^{(p,q)} - \min\left(\mathbf{z}^{(p,q)}\right)}{\max(\mathbf{z}^{(p,q)}) - \min(\mathbf{z}^{(p,q)})}, \\ \boldsymbol{\xi} \in \{\mathbf{X}, \mathbf{Y}\}, \;\; \mathbf{z}^{(p,q)} \in \{\mathbf{x}^{(p,q)}, \mathbf{y}^{(p,q)}\}.\end{gathered} \tag{4}$$

This scaling ensured that all datasets had a comparable range, greatly improving the performance, learning speed, and convergence of the GRNN model, as well as the stability of its outputs. The normalized **X** and **Y** data were then arranged into two-level nested data structures of the type of single-line cell arrays of the form

$$\begin{gathered}Z = \left[\left\{\left[\mathbf{z}_{\mathrm{M}}^{(p,q)}\right]_{q=1}^{Q}\right\}_{p=1}^{P}, \;\; \left\{\left[\mathbf{z}_{\mathrm{T}}^{(p,q)}\right]_{q=1}^{Q}\right\}_{p=1}^{P}\right] \in \left(\left(\mathbb{R}^{n_q \times d}\right)^{1\times Q}\right)^{1\times 2P}, \\ d = \begin{cases} 2, & \text{if } \mathbf{z}^{(p,q)} = \mathbf{x}^{(p,q)} \\ 1, & \text{if } \mathbf{z}^{(p,q)} = \mathbf{y}^{(p,q)}, \end{cases}\end{gathered} \tag{5}$$

from which they were subsequently selected for further analysis.

2.3. GRNN modeling

GRNN is an ANN with a feedforward, memory-based architecture and dynamic structure [10], which is characterized by high nonlinear mapping capability, noise robustness, and low training time requirements. Compared to traditional ANNs [15-18], the GRNN learns in a single-pass manner directly from the training data, thus eliminating repeated iterations and the risk of becoming stuck in local minima [10]. Its theoretical basis is the Parzen-Rosenblatt estimation of the joint probability density function of input-output pairs (X,Y) with a Gaussian kernel in the form of a radial basis function (RBF):

$$\psi_i(\mathbf{X}, \mathbf{X}_i) = \exp\left(-\frac{D_i^2}{2\sigma^2}\right), \tag{6}$$

which leads to an approximation of the conditional mean value of the target variable Y with respect to the input vector **X** expressed by the relation:

$$Y(\mathbf{X}) = \frac{\sum_{i=1}^{I} Y_i \exp\left(-\frac{D_i^2}{2\sigma^2}\right)}{\sum_{i=1}^{I} \exp\left(-\frac{D_i^2}{2\sigma^2}\right)}, \quad D_i^2 = \sum_{j=1}^{J} \left(X_j - X_{ij}\right)^2, \tag{7}$$

where D_i^2 is the square of the Euclidean distance between the input X_j and the i-th value of the training sample X_{ij}; I and J are the number of training and input samples, respectively; and σ is the spread parameter (the width of the function ψ_i), which determines the smoothness of the approximation [19, 20].

The GRNN architecture consists of four interconnected layers [10]:

- The input layer receives input data **X** and distributes it to the pattern layer;
- The pattern layer uses the RBF function (6) to compute the similarity between the current input **X** and each training sample $\mathbf{X}_i$;
- The summation layer computes a weighted S_N and an unweighted sum S_D

$$S_N = \sum_{i=1}^{I} Y_i \psi_i, \quad S_D = \sum_{i=1}^{I} \psi_i; \tag{8}$$

- The output layer generates the predicted output as the ratio of these two sums of the summation layer outputs in the form of regression (7).

The schematic diagram of the proposed GRNN model is shown in Figure 1.

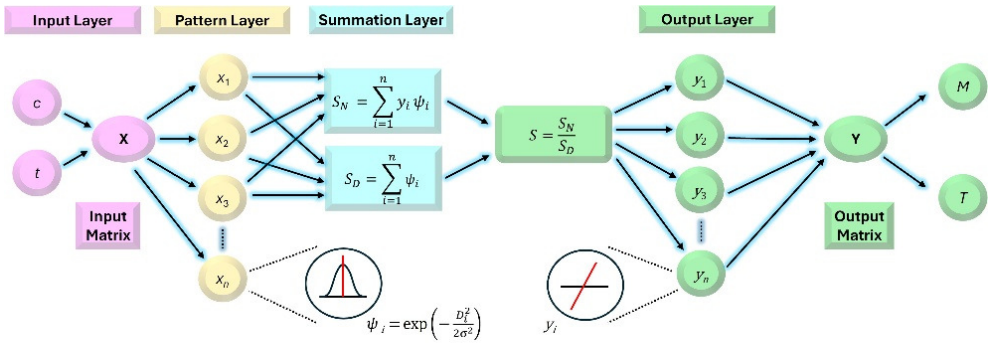

Fig. 1. Schematic diagram of the proposed GRNN model

2.4. GRNN training

The GRNN serves as an approximator of the nonlinear relationships $\hat{\mathbf{Y}}$ between torque **M**, temperature **T**, mixing time **t** and concentration C of the corresponding CB type in the blend, which can be formally expressed in the form of a function:

$$\hat{\mathbf{Y}} = \mathrm{GRNN}_{\sigma}(\mathbf{X}, \mathbf{Y}, \sigma), \quad \hat{\mathbf{Y}} \in \{\mathbf{M}, \mathbf{T}\}. \tag{9}$$

Training the GRNN is an iterative process for finding the optimal value of σ at which the maximum approximation accuracy and model performance are achieved. For this purpose, k-fold cross-validation was used in which the input and target data were divided into k equivalent parts (folds). The model is then repeatedly trained in k iterations, in each of which it is learned on k–1 parts and validated on the remaining one. In doing so, each part serves as a validation set only once, ensuring that all the data are used for both training and validation, leading to a better estimation of the generalization ability of the model.

The training of the GRNN is directed towards optimizing σ, where its optimum is sought on an interval of i positive real numbers $\langle \sigma_{min}, \sigma_{max} \rangle$ not exceeding 1 [21-24]. The optimization was based on minimizing the error quantified using the root mean squared error (RMSE) metric. The optimal value of σ^* is at which the average RMSE across all folds is minimum, where the optimization criterion can be expressed in the form [12]:

$$\sigma^* = \arg\min_{\sigma_i} \left(\frac{1}{k} \sum_{j=1}^{k} \mathrm{RMSE}\left(\mathbf{Y}^{(k)}, \widehat{\mathbf{Y}}\left(\mathbf{X}^{(k)}, \sigma_i \right) \right) \right). \tag{10}$$

The range of the interval $\langle \sigma_{min}, \sigma_{max} \rangle$ with the number of elements i = 1, 2, ... n was determined to minimize the RMSE and simultaneously limit the risk of overfitting when generalizing to new data [21-24].

3. Results and discussion

3.1. Experimental results

The experimental mixing curves of the investigated rubber blends based on the NR matrix in the form of a functional dependence of torque and temperature on mixing time for different types of CB (N121, N339, N550, and N660) and their contents in the blend (45, 50, 55, and 60 phr) are presented in Figure 2.

From Figure 2, it can be seen that all torque curves show an initial step increase owing to the high viscosity of the matrix, which resists the speed of the mixer impellers. Thereafter, there was a smooth decrease owing to the heating of the matrix and the application of shear forces. The torque maxima increased with the stiffening effect of CB in the order N660 < N550 < N339 < N121 and with their content from 45 to 60 phr. The N121 filler showed the most pronounced increase and differences between the contents, whereas for N660, these differences were minimal. After reaching the maximum, the torque decreases owing to the dispersion of the fillers; the higher the filler content, the more pronounced the decrease.

The addition of stearic acid (SA) causes the typical "V" effect – a sudden drop in torque due to reduced friction of the polymer chains, followed by a partial increase. This effect was most pronounced at N121 and 60 phr. The curing system (TBBS and sulfur) induced another "V" effect, caused by the release and re-increase in chamber pressure, not by the properties of the raw materials.

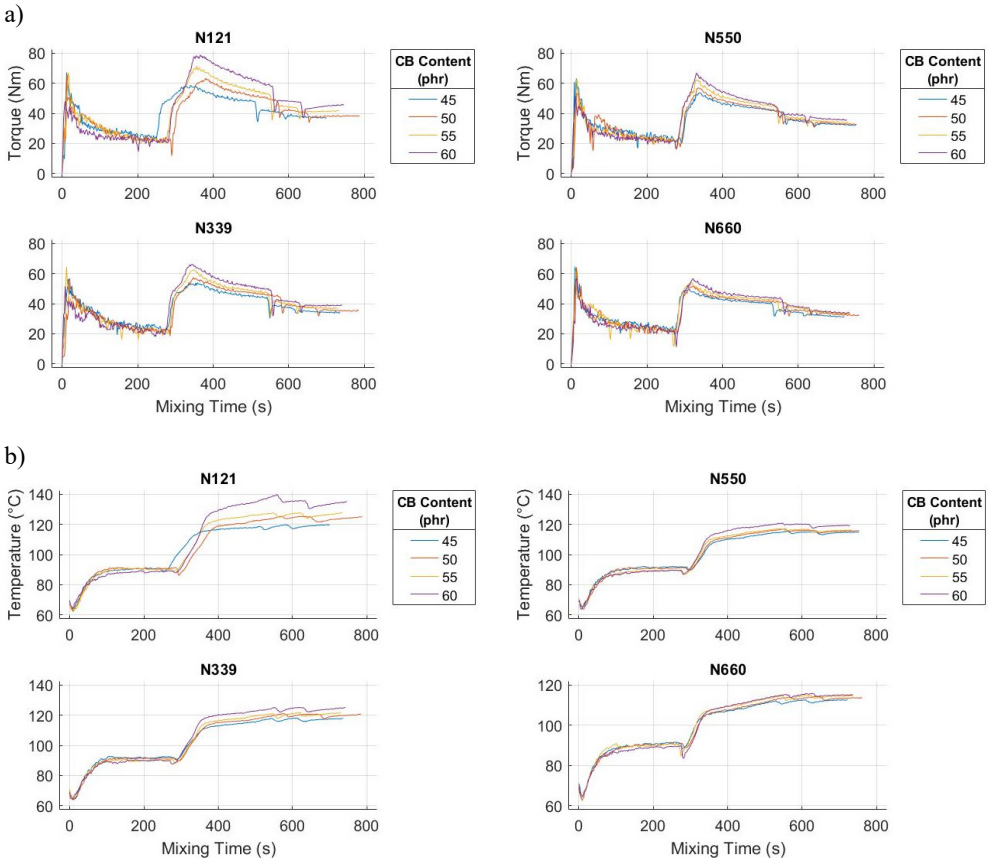

Fig. 2. Experimental mixing curves of: a) torque, b) temperature for different types and contents of carbon black in the blend

The blend temperature curves reflect the same inlet temperature of the matrix, with the initial drop due to the laboratory temperature. The temperature subsequently increases owing to matrix heating, shear forces, and the addition of CB, with the intensity depending on its type and content. The filler N121 at 60 phr achieved the highest temperature increase. After CB dispersion, the temperature increases further owing to the heat build-up and thermal inertia of the chamber.

The addition of SA causes a short-term temperature decrease owing to reduced friction, while the effect is only sustained at N121 and 60 phr – owing to the low matrix fraction and high filler content. Other combinations did not exhibit this effect.

Due to the complex, nonlinear nature of torque and temperature profiles, influenced by CB type, concentration, and physical-chemical changes during mixing, classical analytical models face difficulties in accurate description. Therefore, a GRNN was used to effectively capture the process dynamics from experimental data without

explicit physical modeling, enabling reliable simulation of mixing curves and accurate approximation of real data.

3.2. GRNN training and simulation results

During the training of the GRNN, an optimal spread parameter ($\sigma^* = 6\times10^{-4}$) was identified and subsequently used to retrain the network on the full set of pre-processed training data. The model was then employed to simulate the torque-temperature time histories corresponding to the same inputs it had been trained on, enabling validation of its capability to reconstruct the mixing dynamics and quantify approximation accuracy with respect to the experimental curves.

A comparison between the experimental mixing curves of the investigated rubber blends and their simulated counterparts generated by the GRNN model is presented in Figures 3 and 4.

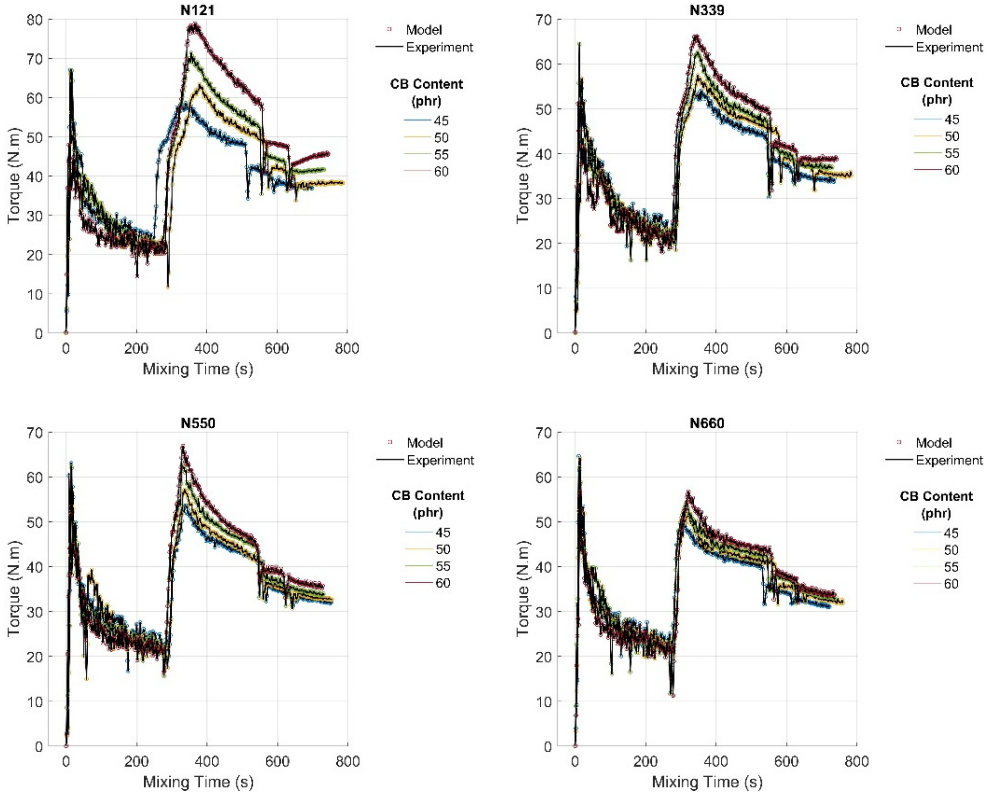

Fig. 3. Comparison of experimental and GRNN-simulated torque curves for the investigated rubber blends at different filler types and loadings

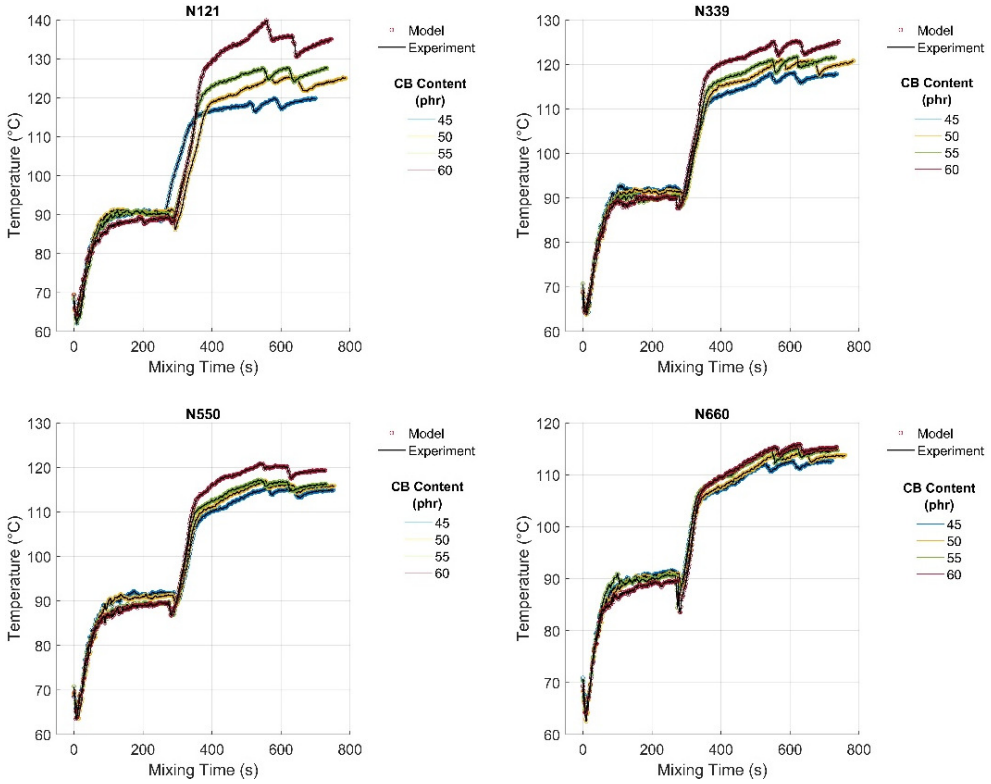

Fig. 4. Comparison of experimental and GRNN-simulated temperature curves for the investigated rubber blends at different filler types and loadings

3.3. Model reconstruction accuracy and prediction analysis

A quantitative analysis of the reconstruction ability and prediction accuracy of the GRNN model was performed using statistical metrics computed on the complete training dataset, namely RMSE and coefficient of determination (R^2) [19]:

$$\mathrm{RMSE} = \sqrt{\frac{1}{n}\sum_{i=1}^{n}(y_i - \hat{y}_i)^2}, \quad R^2 = 1 - \frac{\sum_{i=1}^{n}(y_i - \hat{y}_i)^2}{\sum_{i=1}^{n}(y_i - \overline{y_i})^2}, \tag{11}$$

where y_i is the true value, $\hat{y}_i$ is the predicted value obtained from the model, and $\overline{y_i}$ is the arithmetic mean of true values.

The results of the statistical metrics analysis showed that all the R^2 values were very close to 1, indicating the excellent ability of the GRNN model to capture the variability of the dependent variables with respect to the respective input parameters. This result also confirms the effectiveness of the choice of the optimization interval $\langle \sigma_{min}, \sigma_{max} \rangle$, minimizing the risk of both overfitting and underfitting. The average

RMSE values reached $RMSE_M = 3.569\times10^{-4}$ for the torque and $RMSE_T = 6.686\times10^{-4}$ for the blend temperature, indicating that the average deviation of the predictions from the real values represented only a negligible fraction of the entire range of normalized data. The results confirm that the proposed model is capable of highly accurate reconstruction of the dynamics of the mixing process, which makes it a promising tool for the intelligent modeling of complex dynamic processes in relevant applications with defined input conditions.

Although the results confirm the high reconstruction accuracy of the model on known inputs, its generalization performance on new and unknown data will be the subject of further research.

4. Conclusion

This study presents the first systematic application of GRNN to model the effect of the type and carbon black content on the mixing dynamics of rubber blends. The model was trained on 16 variants of natural rubber-based blends with four CB types (N121, N139, N550, and N660) and concentrations of 45, 50, 55, and 60 phr, respectively. The input variables were the mixing time and concentration of each CB filler, and the GRNN accurately predicted the key mixing characteristics of torque and temperature. Optimization was performed using 10-fold cross-validation to eliminate the risk of overfitting and maximize the generalization capability.

The proposed GRNN model achieved excellent results in reconstructing the torque and temperature waveforms during each mixing cycle, with average RMSE values of $\sim10^{-4}$ and R^2 practically equal to one. These results confirm the high accuracy in capturing the nonlinear relationships between the filler type and content and the observed process variables. Although the model was tested on the same data used for training, it demonstrated its ability to reliably simulate the complex trajectories of the observed mixing parameters. This property allows its practical use in the analysis and optimization of mixing operations, particularly in cases where the mathematical description is insufficient or ineffective.

Owing to the flexibility and scalability of GRNN, the proposed model is suitable for a wide range of conditions and allows for efficient simulation, analysis, and optimization of various technological processes. Future research should focus on extending it to other types of fillers and rubbers as well as the validation of process data to verify the robustness and versatility of the approach.

Acknowledgments

This research was supported by the Operational Programme Integrated Infrastructure – project CEDITEK II (ITMS2014+ code 313011W442), and by the Scientific Grant Agency of the Ministry of Education, Science, Research and Sport of the Slovak Republic under grant number VEGA 1/0691/23.

References

[1] Dick, J.S., & Pawlowski, H. (2023). *Practical Rubber Rheology and Dynamic Properties*. Hanser.

[2] Wypych, G. (2021). *Handbook of Filler*. ChemTec Publishing.

[3] Ghoreishy, M.H.R. (2016). A state-of-the-art review on the mathematical modeling and computer simulation of rubber vulcanization process. *Iran Polymer Journal*, *25*(1), 89-109. DOI: 10.1007/s13726-015-0405-5.

[4] Hammad, M.M. (2024). *Artificial Neural Network and Deep Learning: Fundamentals and Theory*. Convex.

[5] Bratina, M., Šušterič, Z., Šter, B., Lottič, U., & Dobnikar, A. (2009). Predictive control of rubber mixing process based on neural network models. *KGK Kautsch. Gummi Kunstst.*, *62*(7), 378-382.

[6] Golmohammadi, M., & Aryanpour, M. (2023). Analysis and evaluation of machine learning applications in materials design and discovery. *Materials Today Communications*, *35*, 105494. DOI: 10.1016/j.mtcomm.2023.105494.

[7] Bahiuddin, I., Mazlan, S.A., Imaduddin, F., Shapiai, M.I., & Ubaidillah Sugeng, D.A. (2024). Review of modeling schemes and machine learning algorithms for fluid rheological behavior analysis. *Journal of the Mechanical Behavior of Materials*, *33*, 20220309. DOI: 10.1515/jmbm-2022-0309.

[8] Lukas, M., Leineweber, S., Reitz, B., Overmeyer, L., Aschemann, A., Klie, B., & Giese, U. (2024). Minimizing temperature deviations in rubber mixing process by using artificial neural networks. *Rubber Chemistry and Technology*, *97*(3), 371-379. DOI: 10.5254/rct.24.00003.

[9] Park, K., Park, H., & Bae, H.A. (2022). Data-driven recipe simulation for synthetic rubber production. *IEEE Access*, *10*, 129408-129418. DOI: 10.1109/ACCESS.2022.3228241.

[10] Specht, D.F. (1991). A general regression neural network. *IEEE Transactions on Neural Networks*, *2*(6), 568-578. DOI: 10.1109/72.97934.

[11] Al-Mahasneh, A.J., Anavatti, S., Garratt, M., & Pratama, M. (2018). Applications of general regression neural networks in dynamic systems. In: *Digital Systems, IntechOpen*, pp. 133-154. DOI: 10.5772/intechopen.80258.

[12] Kopal, I., Labaj, I., Vršková, J., Harničárová, M., Valíček, J., & Tozan, H. (2023). Intelligent modelling of the real dynamic viscosity of rubber blends using parallel computing. *Polymers*, *15*(27), 3636. DOI: 10.3390/polym15173636.

[13] International Organization for Standardization (ISO). Rubber test mixes – Preparation, mixing and vulcanization: Equipment and procedures; ISO 2393:2014; ISO: Geneva, Switzerland, 2014.

[14] Kim, Y., Kim, M.K., Fu, N., Liu, J., Wang, J., & Srebric, J. (2024). Investigating the impact of data normalization methods on predicting electricity consumption in a building using different artificial neural network models. *Sustainable Cities and Society*, *110*, 105570.

[15] Madhiarasan, M., & Louzazni, M. (2022). Analysis of artificial neural network: Architecture, types, and forecasting applications. *Journal of Electrical and Computer Engineering*, *2022*(12), 1-23, 5416722. DOI: 10.1155/2022/5416722.

[16] Sadollah, A., & Travieso-Gonzalez, C.M. (2020). Recent trends in artificial neural networks from training to prediction. Digital Systems, IntechOpen. DOI: 20.500.12854/67307.

[17] Probert, M. (2021). Machine learning with neural networks: an introduction for scientists and engineers. *Contemporary Physics*, *62*(4), 236-237. DOI: 10.1080/00107514.2022.2038687.

[18] Abdolrasol, M.G.M., Hussain, S.M.S., Ustun, T.S., Sarker, M.R., Hannan, M.A., Mohamed, R., Ali, J.A., Mekhilef, S., & Milad, A. (2021). Artificial neural networks based optimization techniques: A review. *Electronics*, *10*(21), 2689. DOI: 10.3390/electronics10212689.

[19] Helias, M., & Dahmen, D. (2020). *Statistical Field Theory for Neural Networks*. Springer.

[20] Mercioni, M.A., & Holban, S. (2023). A brief review of the most recent activation functions for neural networks. *Proceedings of the 17th International Conference on Engineering of Modern Electric Systems (EMES)*, 1-6. DOI: 10.1109/EMES58375.2023.10171705.

[21] Krzywanski, J., Sosnowski, M., Grabowska, K., Zylka, A., Lasek, L., & Kijo-Kleczkowska, A. (2024). Advanced computational methods for modeling, prediction and optimization – A review. *Materials*, *17*(14), 3521. DOI: 10.3390/ma17143521.

[22] Mahlich, C., Vente, T., & Beel, J. (2024). *e-Fold Cross-Validation for energy-aware Machine Learning Evaluations*. arXiv. DOI: 10.48550/arXiv.2410.09463.

[23] Ghosh, S. (2018). *Kernel Smoothing: Principles, Methods and Applications*. Wiley.

[24] Gambella, C., Ghaddar, B., & Naoum-Sawaya, J. (2021). Optimization problems for machine learning: A survey. *European Journal of Operational Research*, *290*(3), 807-828. DOI: 10.1016/j.ejor.2020.08.045.